

Target-Specific Differences in Somatodendritic Morphology of Layer V Pyramidal Neurons in Rat Motor Cortex

WEN-JUN GAO* AND ZE-HUI ZHENG

Institute of Neuroscience (formerly Shanghai Brain Research Institute),
Chinese Academy of Sciences, Shanghai 200031, China

ABSTRACT

Dendritic geometry has been shown to be a critical determinant of information processing and neuronal computation. However, it is not known whether cortical projection neurons that target different subcortical nuclei have distinct dendritic morphologies. In this study, fast blue retrograde tracing in combination with intracellular Lucifer yellow injection and diaminobenzidine (DAB) photoconversion in fixed slices was used to study the morphological features of corticospinal, corticostriatal, and corticothalamic neurons in layer V of rat motor cortex. Marked differences in the distribution of soma, somal size, and dendritic profiles were found among the three groups of pyramidal neurons. Corticospinal neurons were large, were located in deep layer V, and had the most expansive dendritic fields. The apical dendrites of corticospinal pyramidal neurons were thick, spiny, and branched. In contrast, nearly all corticostriatal neurons were small cells located in superficial layer V. Their apical dendritic shafts were significantly more slender, though spiny like those of corticospinal neurons. Corticothalamic neurons, which were located in superficial layer V and in layer VI, had small or medium-sized soma, slender apical dendritic shafts, and dendrites that were largely spine free. This study indicates that, in layer V of rat motor cortex, each population of projection neurons has a unique somatodendritic morphology and suggests that distinct modes of cortical information processing are operative in corticospinal, corticostriatal, and corticothalamic neurons. *J. Comp. Neurol.* 476:174–185, 2004. © 2004 Wiley-Liss, Inc.

Indexing terms: dendrites; retrograde tracing; corticospinal; corticostriatal; corticothalamic; intracellular injection

Pyramidal neurons are the predominant output neurons of the neocortex and make up 80% of the total cortical neuronal population. These cells are heterogeneous with regard to somal size, somal shape, dendritic branching, spine density, axonal collateralization, and projection site (DeFelipe and Farinas, 1992). Given that specific classes of intrinsic and extrinsic afferents terminate in different cortical layers, the laminar position and dendritic morphology of a neuron will essentially determine the spectrum of inputs impinging on the neuron, as well as neuronal computation of these inputs, and ultimately will influence the propagation of action potentials, coincidence detection, and synaptic plasticity (Larkman and Mason, 1990; Johnston et al., 1996; Magee et al., 1998; Vetter et al., 2001; Benavides-Piccione et al., 2002; Holthoff et al., 2002; Williams and Stuart, 2002, 2003; Hausser and Mel, 2003; Schaefer et al., 2003; Ariav et al., 2003; Konur et al., 2003).

Previous studies have suggested that pyramidal cells in different cortical layers exhibit diverse dendritic morphol-

ogies (Feldman, 1984; Ghosh et al., 1988; Benavides-Piccione et al., 2002; Elston and Rockland, 2002; Konur et al., 2003; Buckmaster et al., 2004). Recently, numerous studies have demonstrated that projection neurons directed to different targets are distinguished by somal size and laminar origin in a number of species, e.g., rat, rabbit, cat, dog, and monkey (Macchi and Bentivoglio, 1986; Wil-

Grant sponsor: National Science Foundation of China; Grant number: 39570244.

Wen-Jun Gao's current address is Department of Neurobiology, Yale University School of Medicine, SHM B403, 333 Cedar St., New Haven, CT 06510.

*Correspondence to: Wen-Jun Gao, Department of Neurobiology, Yale University School of Medicine, SHM B403, 333 Cedar St., New Haven, CT 06510. E-mail: wen-jun.gao@yale.edu

Received 27 March 2002; Revised 28 April 2004; Accepted 28 April 2004
DOI 10.1002/cne.20224

Published online in Wiley InterScience (www.interscience.wiley.com).

son, 1987; McGeorge and Full, 1989; Ebrahimi et al., 1992). Moreover, it is increasingly apparent that, even within a single layer of visual or sensory cortex, pyramidal cells exhibit pleomorphic dendritic arbors and patterns of axonal collateralization that correlate with their projection targets or electrophysiological properties (Katz, 1987; Yamamoto et al., 1987a; Hallman et al., 1988; Hubener et al., 1990; Kim and Connors, 1993; Buckmaster et al., 2004).

As in other neocortical areas, the motor cortex contains pyramidal neurons with highly variable morphologies (Chen et al., 1996; Franceschetti et al., 1998). Corticospinal neurons (PTN) in layer V of cat motor cortex not only have unique morphologic features that correlate with their conduction velocities (Deschenes et al., 1979; Ghosh et al., 1988) but also exhibit distinct distributions of synapses on their dendrites (Liu et al., 1991). Pyramidal neurons in motor cortex also project to other subcortical areas, such as striatum and thalamus, in addition to spinal cord. However, it is not known whether layer V pyramidal cells in motor cortex that project to different subcortical targets differ morphologically with respect to dendritic arborization and spine distribution. In the present study, we investigated the dendritic morphologies and sublaminar distribution of corticospinal, corticostriatal, and corticothalamic neurons (PTN, CSN, and CTN, respectively) in layer V of rat motor cortex by means of fluorescent retrograde tracing combined with intracellular injection in fixed brain slices.

MATERIALS AND METHODS

Surgery and perfusion

This study is based on the results obtained from 30 adult male Sprague-Dawley rats weighing 200–300 g. Twenty-four animals were injected with fast blue (FB; Sigma, St. Louis, MO) in one of three subcortical sites to label PTN, CSN, or CTN, respectively. For the injection surgery, the rats were anesthetized with sodium pentobarbital (Nembutal; 42 mg/kg body weight, i.p.), and the heads were immobilized in a stereotaxic apparatus. Injections into the caudate-putamen nucleus (CPu) and the parafascicular nucleus of the thalamus (Pf) were based on coordinates from the atlas of Karl Zilles (1985). All FB injections were delivered via a glass pipette attached to a 1.0- μ l Hamilton syringe and were infused over a period of 10–20 minutes. 1) For PTN injections, FB (3%, 0.1–0.3 μ l) was injected into the lumbar enlargement of spinal cord. 2) For CSN injections, a lateral approach was used for the CPu injections to avoid dye pollution of the motor cortex. A small opening was made in the left side of the cranial bone above the parietal cortex. FB (3%, 0.1 μ l) was pressure injected into dorsolateral portion of the CPu (AP 0–1 mm, DV 4–5 mm, RL 3.0 mm to bregma). 3) For CTN injections, a direct vertical approach was used to inject FB (0.05 μ l, 3%) into the Pf (AP 4.2, RL 1.1, DV 6.0 mm to bregma). After all injections, the needle was maintained in situ at least 5–10 minutes to prevent FB leakage along the pathway of the needle. The glass pipette was then withdrawn, the incisions were sutured, and the animals were allowed to survive for 3–7 days.

An additional six rats were used for fluorescent double labeling to compare directly the distributions of projection neuron populations within layer V and to determine

whether single pyramidal neurons project to more than one subcortical target area. Pair combinations were PTN-CSN, PTN-CTN, and CTN-CSN. First, 3% FB was injected into CPu; 3 days later, nuclear yellow (1%, 0.05 μ l; Molecular Probes Inc., Eugene, OR) was injected into the lumbar enlargement of the spinal cord or into the Pf, and animals were allowed to survive for an additional 24–40 hours.

The animals were overdosed with sodium pentobarbital intraperitoneally and were perfused through the ascending aorta with 100 ml 0.9% saline to rinse the vascular system, followed by 300 ml fixative [2% paraformaldehyde + 0.1–0.5% glutaraldehyde in 0.1 M phosphate buffer (PB), pH 7.4, 4°C]. The lightly fixed brains were removed and stored in 10% sucrose-PB solution overnight at 4°C.

Histology and intracellular injection with Lucifer yellow

The brains were cut on a Vibratome (Oxford) into alternating 300- μ m-thick slices and 50- μ m-thick sections in a plane orthogonal to the gyrus and parallel to the dendritic orientation of pyramidal neurons. One 300- μ m slice was cut for intracellular injection of Lucifer yellow (LY; see below) followed by two 50- μ m sections that were mounted on slides to localize the FB injection site and to photograph cells retrogradely labeled with FB. This pattern of one thick and two thinner sections was repeated throughout the motor cortex. The 50- μ m sections were counterstained with cresyl violet to determine the laminar distribution of retrogradely labeled neurons. The brains used for fluorescent double labeling were serially sectioned at 30 μ m in the same orthogonal plane and mounted on gelatin-coated slides, then directly observed under an Olympus BX70 epifluorescence microscope and photographed.

The method used for intracellular injection of LY (provided by Dr. W. Stewart) in fixed slices has been reported elsewhere (Buhl and Lubke, 1989; Gao et al., 1996). In brief, while slices were visualized under a Leitz epifluorescence microscope (Leica Microsystems, Wetzlar, Germany), LY (4%) was infused into the FB-labeled cells with a negative DC current of 1–5 nA for 5–20 minutes via a glass pipette (tip diameter <1 μ m). LY rapidly diffused into neuronal soma and dendrites. Successful injection was characterized by complete filling of the dendritic arbor, including small-caliber (<1 μ m) dendrites and spines. The slices were then immersed in diaminobenzidine (DAB) solution [dissolved in 0.05 M Tris buffer (TB), pH 8.2] for 2–5 minutes and irradiated for 15–30 minutes with LY excitation wavelengths (430–490 nm) until all visible fluorescence had faded and the brown DAB reaction had product formed. Excess DAB was washed out with several rinses in phosphate buffer (PB). The slices were mounted on gelatin-soaked slides, air dried, dehydrated in an ascending series of ethanols, cleared in xylene, and coverslipped with neutral resin.

Data analysis

All morphological measurements of DAB-photoconverted neurons were performed at $\times 500$ magnification under a Leitz brightfield microscope unless otherwise stated. Two measurements of somal size were taken, somal width and somal height. The latter was measured from the bottom of the soma to the point where the soma

joined the primary apical dendrite (Yamamoto et al., 1987a). Reconstruction of the injected neurons was performed with the aid of camera lucida drawing tube. The cortical laminar location of LY-injected cells and FB-labeled cells was determined by comparison with adjacent, cresyl violet-stained sections. The areal extent of the basal, oblique, and apical dendritic fields was defined as illustrated in Figure 1. All measurements of the dendritic fields were processed through a computer-assisted Complot 7,000 digitizer from the camera lucida-drawn cells described above and were further analyzed with the Sholl (1953) method.

Detailed analyses of spine distributions were performed on neurons drawn under a $\times 100$ oil-immersion lens with the aid of a camera lucida at a total magnification of $\times 1,250$. All neurons were drawn for arbitrary classification of spine density: neurons were classified as spine dense (≥ 20 spines/50 μm), spine sparse (< 20 spines/50 μm), and spine free. Some spine-free neurons were additionally classified as "probable" if only a few profiles were observed that could not be definitively identified as spines. For analysis of spine distribution, the two most spine-dense neurons from each projection population were selected, and three oblique dendrites, three basal dendrites, and the apical dendritic trunk of each of these neurons were analyzed. The number of spines along each 10- μm dendritic segment was counted for oblique and basal dendrites; the number of spines along each 50- μm dendritic segment was counted for apical dendrite shafts. Corrections were not made for tissue shrinkage during histological processing nor for spines hidden by the dendritic shaft. Axonal staining was not complete or consistent enough with this methodology to allow morphologic comparison of the three projection neuron populations.

Statistical analysis

Pearson's correlation analysis was performed on all relevant pairs of parameters in each of the three projection-specific populations; parameters included somatic size, somatic cut area, apical dendritic length, stem number of oblique and basal dendrites, and dendritic field areas. A two-way ANOVA, or rank sum test for the samples with great variance, was used to test for statistical significance. All measurements are expressed as means \pm SD.

RESULTS

In total, 87 neurons were injected intracellularly and photoconverted by DAB; however, detailed morphometric analysis was limited to the 44 completely filled cells. The remaining cells, which had truncated dendritic profiles, were eliminated from the data set.

Areal and laminar origin of subcortical projection neurons

PTN had large soma that were found in a well-defined, dense band in contralateral Vb. Most labeled cells were distributed in the rostral part of lateral agranular cortex (Agl; the primary motor cortex; Zilles, 1985). Fewer cells were located in medial agranular cortex (Agm) and in secondary somatic sensory cortex (SII; Fig. 2A, Table 1). In contrast to PTN, CSN were significantly smaller ($F = 298.2$, $P < 0.001$) and were found predominantly in ipsi-

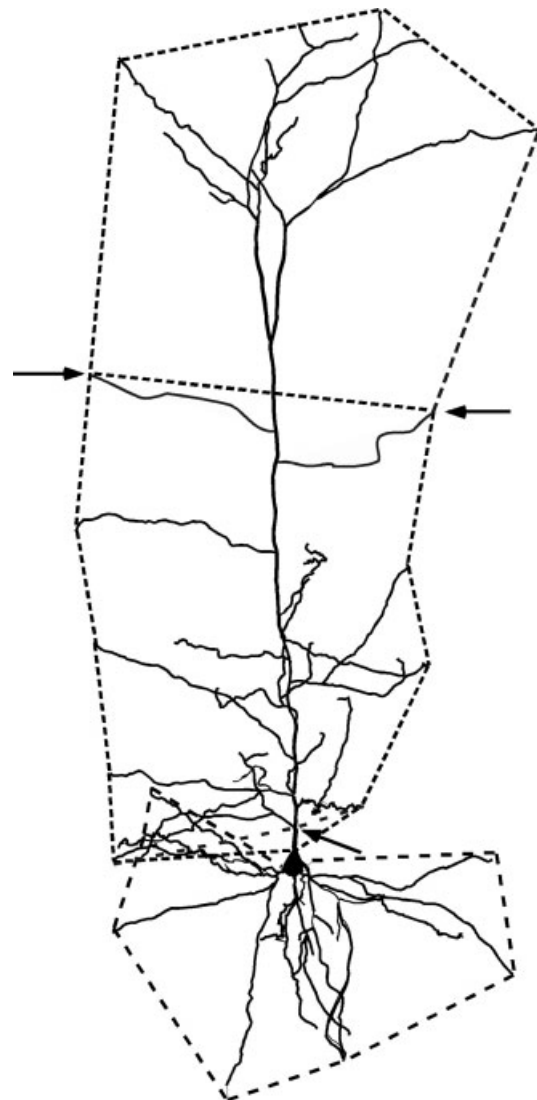


Fig. 1. Drawing illustrating the neuronal landmarks used to determine the areal extent of apical, oblique, and basal dendritic fields. The apical dendritic field was defined as a polygon whose top was formed by lines connecting the distal tufts, whose sides were formed by lines connecting the tips of the oblique dendrites and whose base was formed by a line intersecting the stem of the apical dendrite. A similar polygonal area represented the oblique dendritic field; the sides of this field were also defined by lines connecting the tips of the oblique dendrites and base by a line intersecting the stem of the apical dendrite. However, the top was defined by a line intersecting the tips of the distal-most oblique dendrites (line indicated by arrows). The basal dendritic field formed an area beneath the soma that was defined by connecting all the points represented by the distal tips of the basal dendrite with the line formed by the base of the pyramidal cell soma (area below soma).

lateral prefrontal cortex and motor cortex (Table 1). However, both the areal distribution and the relative number of labeled cells varied with the locus of the striatal injection. In the prefrontal cortex, densely labeled CSN spanned laminae II–VI, whereas, in primary motor cortex, most cells were located in Va, with a few found in IIIc bilaterally (Fig 2B). CTN soma were significantly smaller

than PTN soma ($F = 288.9$, $P < 0.001$) and were observed in both layers Va and VI contralaterally (Fig. 2C,D, Table 1). Significant differences were found in the average depth

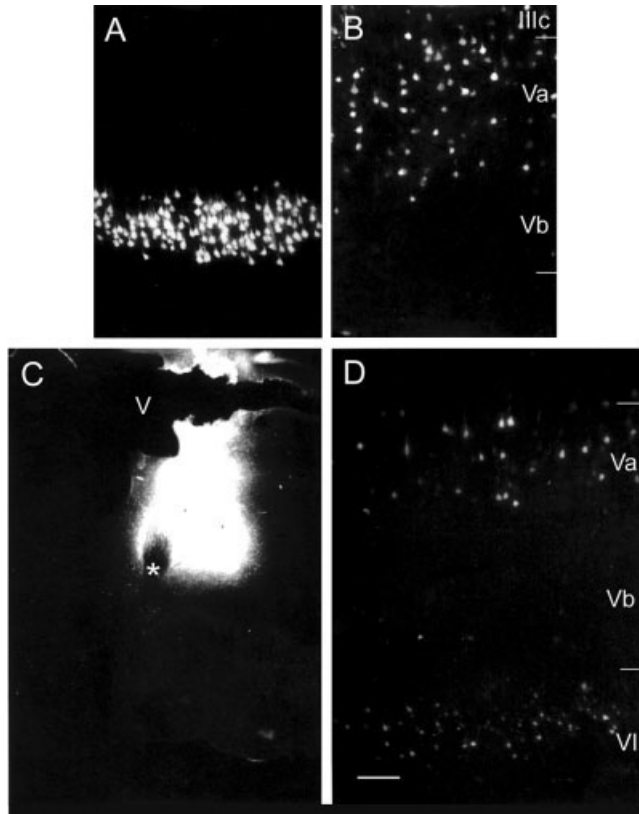


Fig. 2. Photomicrographs of retrogradely labeled fluorescent PTN, CSN, and CTN showing the laminar distributions in the contralateral motor cortex after injection of FB in the lumbar spinal cord, dorsolateral part of caudate-putamen nucleus, and parafascicular nucleus of thalamus (injection site also shown), respectively. **A:** PTN were heavily labeled in a dense, compact band in deep layer V (Vb). **B:** In contrast, CSN were dispersed throughout the superficial part of layer V (Va) and extended into deep layer III (IIIc). **C:** The injection site of FB in the parafascicular nucleus of thalamus appears as a teardrop-shaped white area. The fasciculus retroflexus (asterisk) and the lateral ventricle (V) are indicated for anatomic orientation. **D:** The vast majority of retrogradely labeled CTN cells were located in layers Va and VI. Scale bar = 200 μm in D (applies to A,B,D); 400 μm for C.

from the pial surface between PTN and CSN ($P < 0.01$) and between PTN and CTN ($P < 0.05$). CSN and CTN did not differ from each other in laminar depth or somal size (Table 1).

Fluorescence double labeling failed to show any double-labeled PTN-CSN or PTN-CTN cells in the motor cortex. However, a few (<5%) double-labeled CTN-CSN neurons were found. This finding is consistent with the overlapping distribution of CTN and CSN in Va of motor cortex (data not shown).

Dendritic morphology of subcortical projection neurons

Apical dendritic shafts. PTN had thick apical dendrites that tapered gradually in an ascending course toward the pial surface. Many (9/16, 56%) bifurcated two to four times at variable positions within layer III, generally within 300 μm of the soma, and in so doing gave rise to multiple, parallel dendritic trunks that terminated in several small, horizontally oriented tufts in layer I (Figs. 3A, 4A, 5, Table 1). In comparison with PTN, CSN had thinner apical dendritic shafts that changed very little in diameter in their traverse to the pial surface (Figs. 3B, 4B, 5). The majority of CSN shafts did not bifurcate. As with CSN, most CTN were also characterized by thin apical dendritic shafts of a relatively homogeneous diameter that did not bifurcate (Figs. 3D, 5, Table 1).

Quantitative comparison of apical dendritic features among the three groups revealed that PTN had a significantly larger diameter of apical dendritic shafts at 100 μm from the soma relative to CSN ($F = 46.624$, $P < 0.005$) or CTN ($F = 93.126$, $P < 0.001$; Table 1), with no difference between CSN and CTN ($F = 1.664$, $P = 0.238$). Consistently with the depth of their soma relative to the pial surface, PTN had the longest average apical dendritic lengths, CSN had the shortest, and CTN apical dendrites were intermediate in length (Figs. 6, 8A). Apical dendritic lengths were not correlated with somatic sizes or somatic cut areas for any of the three populations.

Oblique dendrites. The stem numbers of oblique dendrites and their spatial expanse were very similar for the three populations of neurons (Table 1, Fig. 4; note, however, that the CTN shown in Fig. 4C is atypical in having few oblique dendrites). Generally, oblique dendrites branched from the apical shaft in layers V and III above the cell body. Although the longest of these branches was

TABLE 1. Somatodendritic Morphology of Subcortical Projection Neurons in the Motor Cortex

	PTN (n = 16)	CSN (n = 13)	CTN (n = 15)	Statistics
Layers of origin	Vb	Va, IIIc	Va, VI	
Depth of soma (μm)	824.1 \pm 169.28	601.7 \pm 241.77	713.7 \pm 164.41	a ² , b ¹
Soma size (μm)	21.2 \pm 2.63 \times 25.2 \pm 3.87	15.7 \pm 2.22 \times 16.2 \pm 5.19	15.5 \pm 2.36 \times 18.9 \pm 3.48	a ³ , b ³
Somatic cut area (μm^2)	536.0 \pm 123.38	253.0 \pm 83.62	294.6 \pm 79.11	a ³ , b ³
Number of AD bifurcations	9	0	1	
Diameter of AD 25 μm to soma	6.9 \pm 0.83	3.5 \pm 0.99	4.1 \pm 1.04	a ³ , b ³
Diameter of AD 100 μm to soma	4.2 \pm 0.63	2.8 \pm 0.64	2.6 \pm 0.76	a ² , b ³
Stem number of OD	8.8 \pm 2.27	7.5 \pm 2.30	7.9 \pm 2.83	
Stem number of BD	5.2 \pm 1.28	7.3 \pm 1.65	5.3 \pm 1.63	a ³ , c ³
Number of terminal tips of BD	3.9 \pm 2.39	2.8 \pm 1.46	4.4 \pm 1.57	a ² , c ³
Dendritic field of AD (μm^2)	54,500 \pm 19,500	40,900 \pm 10,800	49,800 \pm 19,700	
Dendritic field of OD	45,300 \pm 11,100	40,600 \pm 15,000	42,800 \pm 21,800	
Dendritic field of BD	66,700 \pm 29,200	57,300 \pm 21,300	65,100 \pm 25,700	a ¹

¹ $P < 0.05$.

² $P < 0.01$.

³ $P < 0.001$.

AD, apical dendrite; BD, basal dendrite; OD, oblique dendrite; CSN, corticospinal neurons; CTN, corticothalamic neurons; PTN, corticospinal neurons. a, comparison between PTN and CSN; b, comparison between PTN and CTN; c, comparison between CSN and CTN.

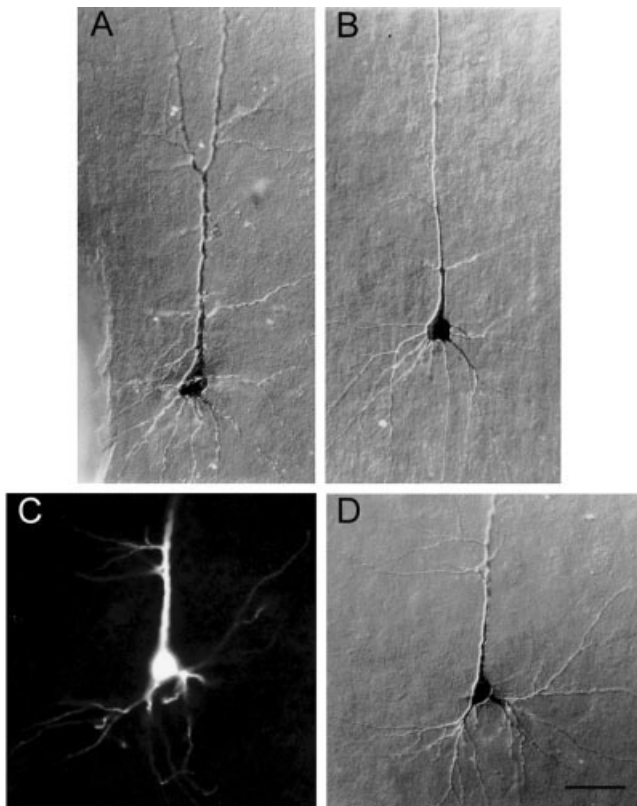


Fig. 3. Photomicrographs of intracellularly LY injected and DAB photoconverted cells in 300- μm -thick slices. **A:** A Nomarski photograph of a DAB photoconverted PTN shows the large cell body and a thick apical dendritic trunk that bifurcates into two parallel apical dendrites. **B:** A typical CSN has a smaller soma and more slender and even-caliber apical dendritic shaft. An LY intracellularly labeled (**C**) and DAB-photoconverted (**D**) CTN is shown to illustrate the small soma and nonbifurcating apical dendrite. Scale bar = 50 μm .

400 μm , their lengths ranged from 50–200 μm (mean $162.9 \pm 37.70 \mu\text{m}$). For all three populations, stem number varied greatly (range 4–12, Table 1) and often had secondary or tertiary order branches, resulting in a total of ~ 16 distal endings or tips. However, some characteristics of oblique dendrites differed among the three pyramidal cell populations. For example, most oblique dendrites on PTN and CTN originated within 200 μm of the soma, whereas oblique dendrites of CSN branched closer to the soma ($\pm 150 \mu\text{m}$). In addition, a significant positive correlation was found between the number of oblique dendrites and the length of the apical dendritic shaft for CSN ($r^2 = 0.648$), but not for PTN ($r^2 = 0.123$) or CTN ($r^2 = 0.224$; Fig. 6).

Basal dendrites. Basal dendrites of the three classes of pyramidal neurons also shared many common features. For instance, the branching pattern, as measured by the number of tips arising from each stem, was highly variable (ranging from 1 to 12) in all three populations, resulting in large standard deviations of the mean value of tips for all three pyramidal classes (Table 1). Most of the branching occurred proximal to the soma, and this differed from the pattern on oblique dendrites (Fig. 7). In

addition, certain characteristics distinguished basal dendrites among the three neuronal populations. PTN and CTN basal dendrites were similar ($F = 1.672$, $P = 0.217$) in morphology but significantly differed from CSN dendrites in having fewer primary “stem” basal dendrites (PTN vs. CSN: $F = 102.4$, $P < 0.001$; CTN vs. CSN: $F = 288.3$, $P < 0.001$) and number of terminal tips (PTN vs. CSN: $F = 6.936$, $P < 0.01$; CTN vs. CSN: $F = 79.3$, $P < 0.001$; Table 1).

Dendritic field area. The basal dendritic fields of PTN were similar to those of CTN ($F = 1.474$, $P = 0.328$) but significantly larger compared with CSN fields ($F = 5.852$, $P < 0.05$; Table 1). In addition, Sholl analysis indicated that the basal dendrites of CSN extended outward only 200 μm from soma, a radial distance shorter than that of either CTN or PTN (Fig. 7A). Apical dendritic field sizes did not differ among three neuronal populations (Table 1), although PTN had significantly longer apical dendrites in comparison with CSN ($F = 6.35$, $P < 0.01$). The lack of a significant difference may indicate that the PTN have longer, but narrower, apical dendritic fields or might be due to the considerable variability among individual neurons. Oblique dendrites of all three pyramidal populations had generally similar areal field sizes and radial expanses (Table 1, Fig. 7).

Spine distribution. The three morphologic classes of spines described previously by Peters and Kaisermann-Abramof (1970), i.e., mushroom-shaped, stubby, and thin spines, were all observed in the present study, although most spines belonged to the thin spine category. Classification of neurons according to spine density as described above revealed that all three populations of neurons had both spine-dense and spine-sparse neurons (Table 2). Only CTN were definitively classified as spine free, and notably spine-free CTN constituted 53.3% (8/15) of all CTN studied, or 66.7% (10/15) of all CTN if probable spine-free neurons were included (Table 2, Fig. 8). In comparison, only two PTN were classified as spine free, and there was some uncertainty about the classification (Table 2).

The general patterns of spine distribution, as assessed in the two most spine-dense neurons in each population, were similar in PTN, CSN, and CTN. The most proximal portions of the apical and basal dendrites were always devoid of spines (Figs. 8F, 9A,C). The length of the spine-free segment on the primary basal dendrite was comparable in the three neuronal populations ($\sim 20 \mu\text{m}$); in contrast, the spine-free segment of the apical dendritic shafts varied greatly in length, with PTN having the longest (50–70 μm), CSN having the shortest ($\sim 20 \mu\text{m}$), and CTN having an intermediate length (30–40 μm) spine-free segment. In all three populations, spine density on apical dendritic shafts increased to a peak density midway between the soma and the distal dendritic tufts and then gradually decreased toward the pial surface (Fig. 8A–C). Likewise, in all three populations of neurons, oblique dendrites were covered with spines. Finally, there was a marked reduction in spine density on oblique branches in layer I, and the distal tips of basal and oblique dendrites had few spines.

In contrast, spine density differed among the three populations of neurons on both basal ($F = 3.214$, $P = 0.055$) and oblique ($F = 62.002$, $P < 0.001$; Fig. 9) dendrites. Comparison of spine densities on basal dendrites among

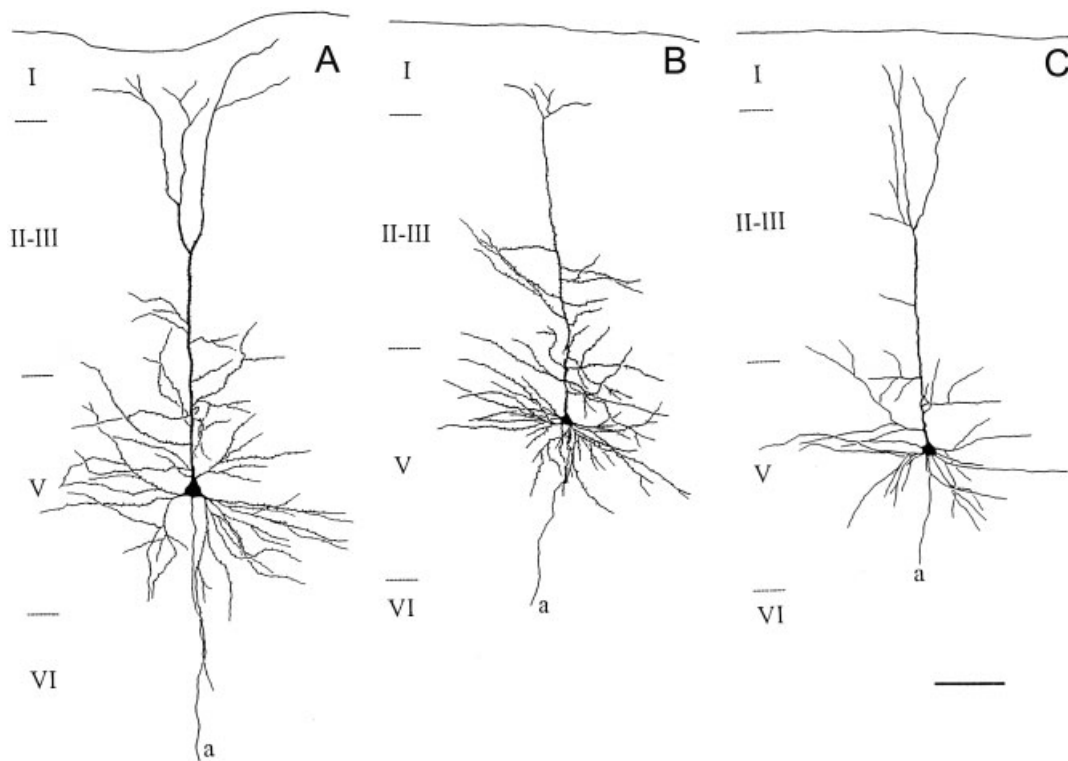


Fig. 4. Representative, camera lucida-drawn PTN, CSN, and CTN. **A:** A typical spiny PTN in deep layer V (Vb) of motor cortex is illustrated. The large soma had a thick apical dendrite that tapered as it ascended toward the pial surface and bifurcated twice to produce three parallel apical dendritic trunks that terminated as small horizontal tufts in layer I. The axon (a) also can be seen clearly. **B:** A CSN with a spine-dense dendritic tree is located in layer Va. These had

small soma and thin apical dendrites that gave off oblique branches in their ascending course to layer I. **C:** An aspiny CTN located in the superficial part of layer V (Va) is shown. These cells were generally small or medium-sized neurons with thin apical dendritic trunks that gave rise to several oblique dendritic branches. The cell illustrated here is not representative of the population as a whole with respect to number of oblique dendrites. Scale bar = 100 μm .

the three groups revealed that PTN and CSN had significantly more spines relative to CTN ($F = 10.034$, $P < 0.01$ and $F = 9.505$, $P < 0.01$, respectively), with no difference between PTN and CSN ($F = 0.425$, $P = 0.525$). Similarly, the spine density on the oblique dendrites of PTN was significantly greater than that of CTN ($F = 10.880$, $P < 0.01$); no significant differences were observed between PTN and CSN ($F = 4.087$, $P = 0.056$) as well as between CSN and CTN ($F = 1.425$, $P = 0.244$).

Though not studied in detail, spine distribution on spine-sparse neurons differed from that of spine-dense neurons for all three populations. The apical dendritic trunks of spine-sparse neurons were nearly devoid of spines, and the primary branches of oblique dendrites on spine-sparse cells had greatly reduced spine density relative to the secondary branches.

DISCUSSION

The somatodendritic morphology of PTN, CSN, and CTN has been revealed in detail by a combination of retrograde tracing and intracellular injection in fixed slices. We uncovered striking differences between PTN and CSN in layers of origin, somal size, and dendritic profiles. CTN more closely resembled CSN but also exhibited some features in common with PTN.

Methodological considerations

The advantages of the techniques used here have been well described elsewhere (Buhl and Lubke, 1989; Hubener et al., 1990). In our study, the intracellular injection method produced nearly complete filling of the dendritic tree, with exception of the axonal processes. In most neurons, dye was observed in fine basal and oblique terminal dendrites (diameter $< 1 \mu\text{m}$) and in spines. In the majority of filled neurons, the apical dendrite extended into layer I and ended in a cluster of small dendritic tufts, in accordance with descriptions of layer V pyramidal cell dendrites from Golgi studies (Feldman, 1984; DeFelipe and Farinas, 1992) and in vivo intracellular injection (Wilson, 1987; Cowan and Wilson, 1994).

One potential drawback of intracellular injection methodology is the need to use thick slices. Only the FB-labeled cells just below the surface of a slice are visible because of the general opaqueness of the tissue. In addition, superficially located perikarya were impaled more easily than those lying deeper in the slice. As a result, some intracellular injections filled only a portion of the dendritic tree, because the remainder of the dendritic arbor was not present within the slice containing the cell body. A systematic error of this nature might interfere with quantitative analysis of neurons in three dimensions, but, for

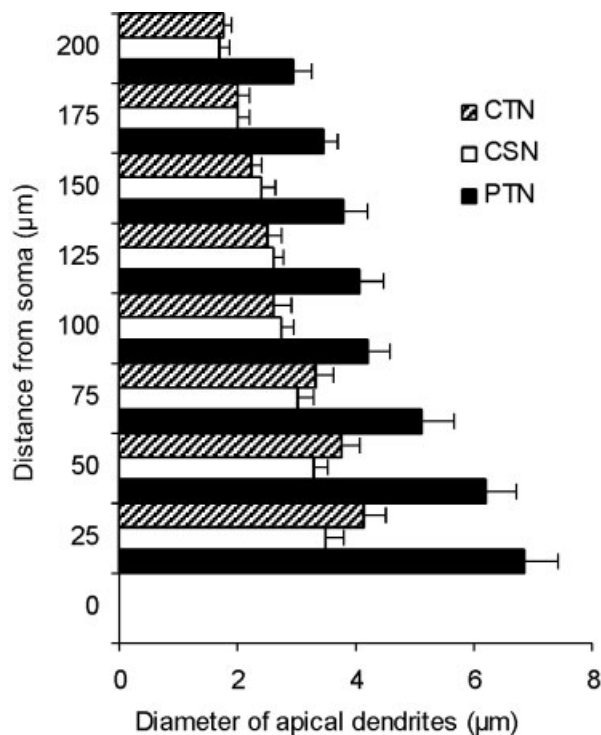


Fig. 5. Comparison of the diameter of apical dendritic shafts in the three cell classes. PTN possessed significantly thicker apical dendrites relative to both CSN ($P < 0.01$) and CTN ($P < 0.001$), which had very slender apical dendrites. The apical dendritic shafts of PTN tapered in the first 100 μm from the soma, whereas apical dendrites of CSN and CTN changed relatively little in diameter.

two-dimensional analyses such as those performed in the present study in which only that portion of the dendritic tree located in the same plane as the cell soma was examined, this error did not significantly affect the results. Moreover, the somatic locations of intracellularly stained PTN, CSN, and CTN were quite comparable to the laminar distributions previously described for a larger sample of cells retrogradely labeled by horseradish peroxidase (HRP; Wise and Jones, 1977). Thus, our sample of intracellularly injected cells was not biased toward larger cells and was representative of the whole population of PTN, CSN, and CTN.

Laminar distribution of projection neurons

PTN were situated contralateral to the injection site in layer Vb and, therefore, did not overlap the more superficially located CSN and CTN neurons in layer Va. The distribution of the three efferent populations of cells in layer V reported here is consistent with findings from tract tracing studies in rat (Wise and Jones, 1977; Catsman-Berrevoets et al., 1980; Catsman-Berrevoets and Kitai, 1981; Miller, 1987), cat (Catsman-Berrevoets and Kitai, 1981), and monkey (Catsman-Berrevoets and Kuypers, 1978). CSN were located in layer III, as well as in layer Va, and were distributed both ipsilateral and contralateral to the injection site. The cells of origin of the crossed corticostriatal projection were of the same size and had the same laminar distribution as those of the ipsilateral cells, as previously reported (Jones et al., 1977; Ger-

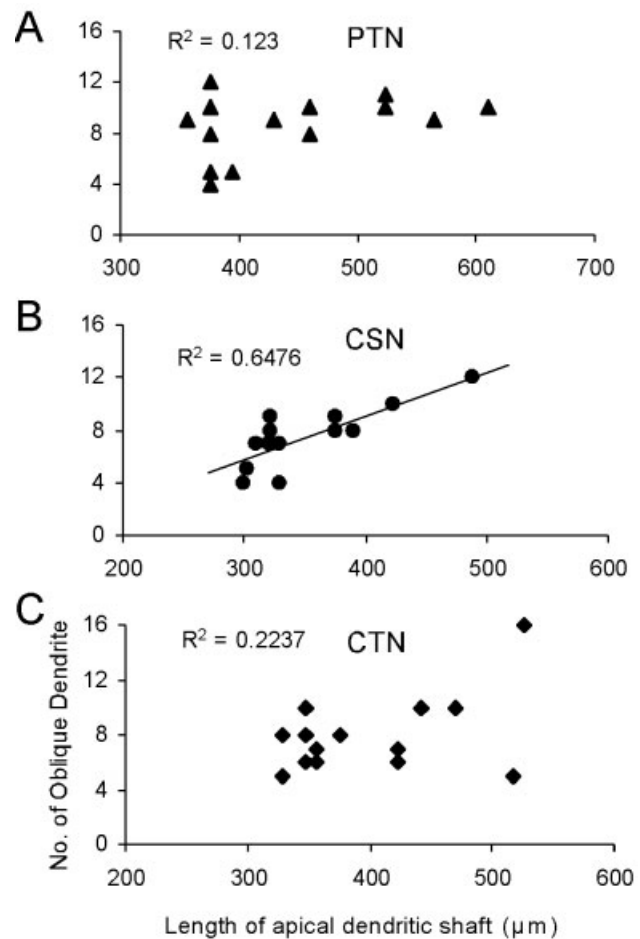


Fig. 6. A positive correlation between the number of oblique dendrite and length of apical dendritic shaft was observed only in CSN (B) and not PTN (A) or CTN (C).

fen, 1989; Akintunde and Buxton, 1992). CTN soma that projected to the Pf nucleus were located mainly in layers VI and Va, in agreement with the results of previous HRP studies in cat (Royce, 1983a; Rouiller and Welker, 2000).

In the present study, only a small percentage of projection neurons was doubly labeled, and all formed collateral projections to the striatum and thalamus, an observation consistent with previous reports of retrograde studies (Catsman-Berrevoets et al., 1980; Donoghue and Kitai, 1981; Wilson, 1987; Royce, 1983b) and results of juxtacellular anterograde labeling (Deschenes et al., 1994; Zhang and Deschenes 1997; Veinante et al., 2000). However, Donoghue and Kitai (1981) also reported that collaterals from corticospinal neurons entered the striatum, a finding that was not corroborated in this study.

Dendritic morphology in relationship to physiological properties

In the motor cortex of cat and monkey, PTN in layer V with fast and slow axonal conduction velocities have been shown to exhibit distinct dendritic characteristics (Deschenes et al., 1979; Landry et al., 1984; Liu et al., 1991; Baranyi et al., 1993). Fast PTN have larger somata than

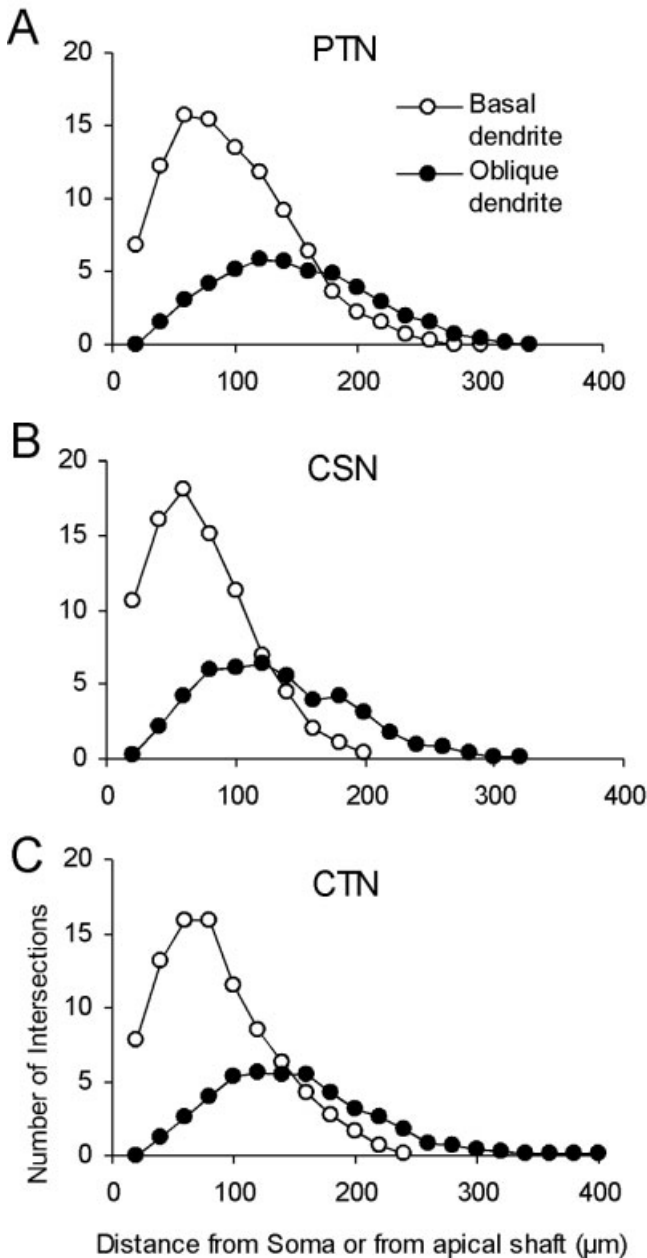


Fig. 7. Sholl plots showing the number of intersections made by PTN (A), CSN (B), and CTN (C) dendrites with a series of concentric circles placed at regularly spaced distances from the soma (for basal dendrites) or from the apical dendritic shaft (for oblique dendrites). The overall pattern of dendritic complexity was similar among the three neuronal populations, although basal dendrites of CSN were generally shorter than those of PTN and CTN.

slow PTN, and their dendritic fields occupy a larger territory in the tangential plane relative to that of slow PTN. Also, dendrites of fast PTN are smooth and devoid of spines, whereas dendrites of slow PTN have a moderate number of spines. Thus, even neurons that belong to the same efferent system may have distinct dendritic morphologies, perhaps reflecting differences in the way in which these cells integrate afferent information. It is note-

TABLE 2. Classification of Projection Neurons Based on Spine Density

	PTN (n = 16)	CSN (n = 13)	CTN (n = 15)
Spine dense (≥ 20 spines/50 μm)	8	4	2
Spine sparse (< 20 spines/50 μm)	6	9	3
Spine free, definite	0	0	8
Spine free, probable	2	0	2

worthy that all of the injected PTN in the present study, with the exception of two that were not definitively classified, belonged to the slow PTN, because all bore spines. This observation is consistent with Cowan and Wilson's study (1994) showing that all PTN in rat had anatomical and physiological properties corresponding to those of slow PTN in cat and monkey (Donoghue and Kitai, 1981).

Intrinsic burst firing is another physiologic property that has been shown to correlate with somatic location and dendritic morphology (Bannister and Larkman, 1995a,b). Neurons in layer Vb in the visual cortex of cat (Hubener et al., 1990) exhibit burst firing and also have large, thick apical dendritic trunks (Church and Baimbridge, 1991). This is consistent with the situation in layer V of the rat neocortex; large cells with long, thick apical trunks were burst spiking, whereas smaller cells with thinner, shorter apical trunks were regularly spiking (Chagmac-Amitai et al., 1990; Mason and Larkman, 1990). Our results indicated that the pyramidal neurons in sublayer Vb of motor cortex had thick apical shafts, whereas those in Va had slender ones. At present, it is not known whether the thick PTN cells of Vb are physiologically burst spiking and the slender CSN and CTN neurons of the Va are regularly spiking neurons.

Insofar as afferents from different intrinsic and extrinsic sources synapse in a lamina-specific fashion, the size and spatial expanse of the dendritic tree influence the integration of excitatory and inhibitory inputs impinging on the neuron (Larkman, 1991a,b; Holthoff et al., 2002; Konur et al., 2003; Buckmaster et al., 2004). Therefore, a detailed description of the neuronal dendritic structure of any given neuronal population is important for the development of models of active and passive summation of synaptic information on the population. In this study, we found that PTN had larger dendritic fields than neighboring CSN and CTN. These findings indicate that PTN might receive more diverse input information from a broader range of intrinsic and extrinsic sources than do CSN or CTN.

Spine distribution

Numerous studies have addressed the possible role of dendritic spines in information processing, synaptic plasticity, and neuroprotection (Harris and Kater, 1994; Segal, 1995, 2002; Yuste and Denk, 1995; Shepherd, 1996; Engert and Bonhoeffer, 1999; Maletic-Savatic et al., 1999; Yuste et al., 2000; Sabatini et al., 2001; Konur et al., 2003). Spine density varied widely in each of the three cell classes in the present study. However, the total numbers of spines on PTN was clearly greater than that of either CSN or CTN, because their spine density was higher and the dendritic arbor was larger. Among the three efferent neuron populations studied, CTN had the fewest spines, and most CTN were devoid of spines. Although this finding contradicts data from Golgi studies indicating that

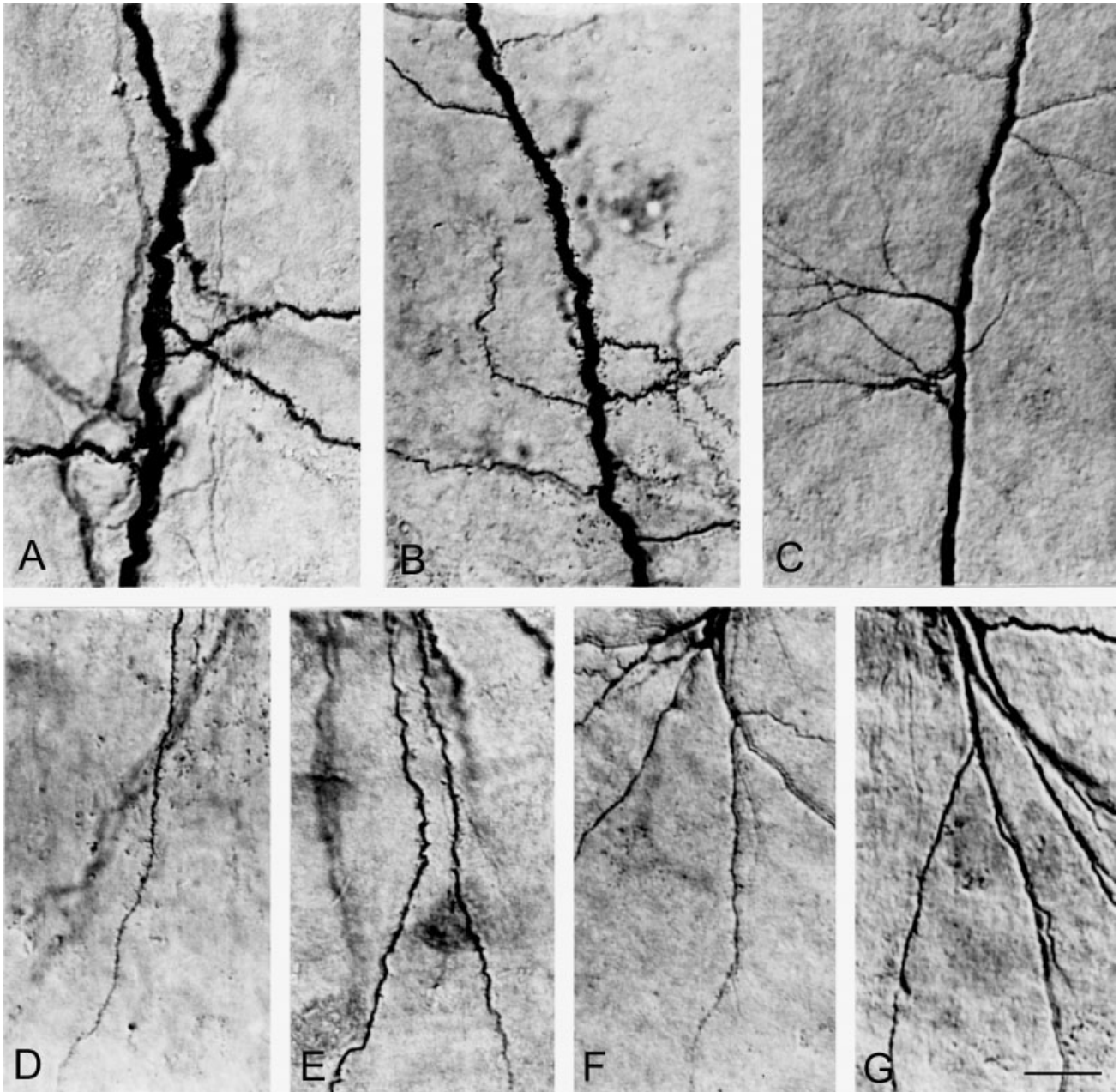


Fig. 8. Photographs showing spine distribution on the midsection of apical dendrites of PTN (A), CSN (B), and CTN (C). Spines were clearly visible on both the apical dendritic shafts and the proximal part of their oblique branches of PTN and CSN but were very sparse

in CTN. Spines on the basal dendrites of PTN (D), CSN (E), and CTN (F) are illustrated. G: Example of a spine-free basal dendrite belonging to a CTN is shown. Scale bar = 25 μm .

spines are present on dendrites of all typical pyramidal cells (DeFelipe and Farinas, 1992), it is in agreement with numerous previous studies using intracellular injection of dyes, which have found some layer V pyramidal cells that were spine-free in monkey and cat motor (Labelle and Deschenes, 1979; Deschenes et al., 1979; Hamada et al., 1981a,b; Liu et al., 1991), cat somatosensory (Yamamoto et al., 1987b, 1990), cat parietal (Samejima et al., 1985; Yamamoto et al., 1987a), and cat visual (Gabbott et al., 1987; Hubener et al., 1990) cortices.

We are aware that spine density measurements in the present study represent an underestimate of true spine density. As is true of most data in the existing literature, our analyses did not take into account tissue shrinkage (Trommald et al., 1995), nor were spine counts corrected for spines that were hidden behind the shaft of the dendrite (Feldman and Peters, 1979). Fixation might also diminish spine counts, in that intracellular injections in living brain slices stains more spines than comparable intracellular injections in fixed slices (Bannister and

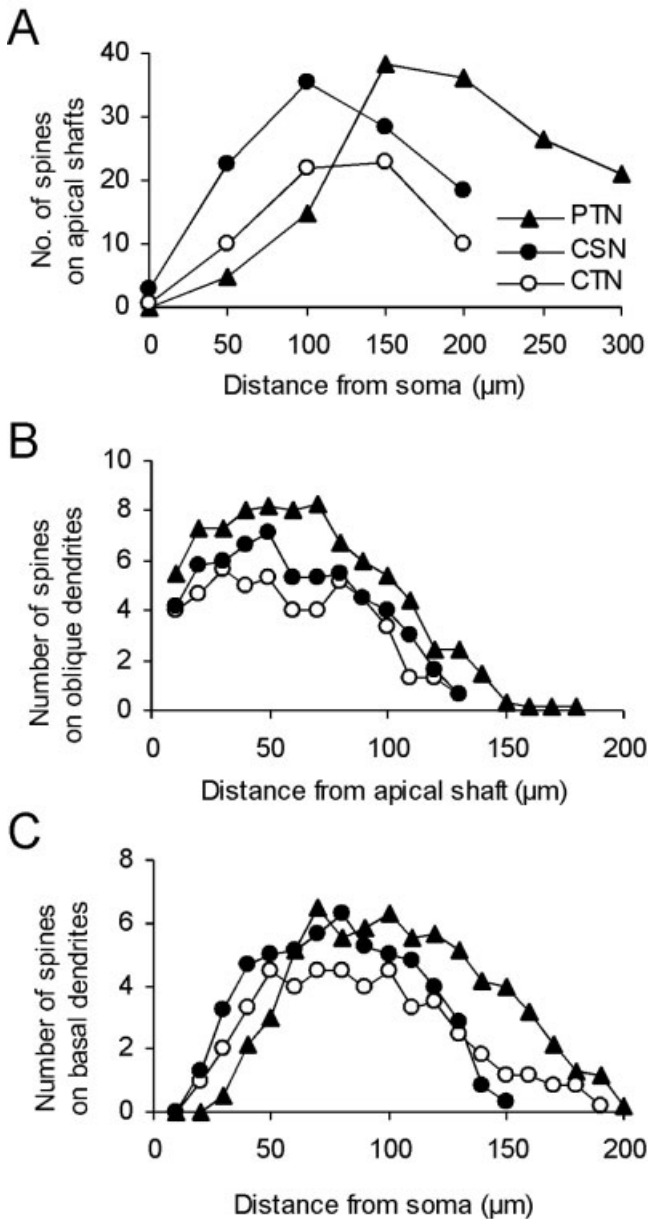


Fig. 9. Spine distribution at regularly spaced distances from the soma (for apical dendritic shafts and basal dendrites) or from the apical dendritic shaft (for oblique dendrites). **A**: There were significantly more spines on apical dendritic shafts of PTN and CSN than on CTN. Moreover, spines on PTN were distributed at a greater distance from the soma than those of CSN or CTN. Spines on oblique (**B**) and basal (**C**) dendrites were distributed mainly in the middle segments in all three populations. PTN had the greatest spine density on oblique and basal dendrites, whereas spine distribution on CTN dendrites was the least dense.

Larkman, 1995a,b), as performed in this study. However, spine density on spine-dense pyramidal neurons in the motor cortex in this study was very similar in magnitude to the measured density based on Golgi stained neurons in the neocortex (DeFelipe and Farinas, 1992). Therefore, we believe that spine staining in fixed slices accurately re-

flects the overall distribution of spines on three classes of projection neurons.

Functional implications

Recent advances in electrical and optical recording techniques have shown that dendritic signaling is a remarkably diverse and dynamic process (Magee et al., 1998; Hausser et al., 2000; Williams and Stuart, 2002, 2003). The varied morphologic, electrical, and chemical properties of dendrites afford a wide spectrum of computational options, which in turn allows individual neurons to carry out specialized functions within their respective networks (Larkum et al., 1999; Hausser et al., 2000; Reyes, 2001; Poirazi and Mel, 2001; Segel, 2002; Hausser and Mel, 2003; Schaefer et al., 2003). In addition, differences in dendritic morphology in part may determine the extent of back-propagation and forward-propagation of action potentials (Vetter et al., 2001; Williams and Stuart, 2003) as well as intrinsic firing patterns (Connors and Gutnick, 1990; Mainen and Sejnowski, 1996). The efficacy of action potential back-propagation in layer V pyramidal neurons correlates with the number and branching pattern of apical oblique branches and the diameter of the apical trunk (Kim and Connors 1993; Schaefer et al., 2003). Therefore, back-propagation of action potentials may occur more frequently in PTN than in other pyramidal cell populations, insofar as these neurons have thick apical dendritic trunks giving rise to many oblique branches. Overall, our finding of target-specific differences in somatodendritic morphology of layer V neurons in motor cortex suggests that corticospinal, corticostriatal, and corticothalamic neurons have distinct capabilities with respect to integration and processing of afferent information, because even subtle differences in dendritic structure may contribute substantially to neuronal function (Mainen and Sejnowski, 1996; Schaefer et al., 2003).

ACKNOWLEDGMENTS

The authors thank Mr. J.B. Mao for expert technical assistance; Mr. Q. Lan for photography; and Sir X.-T. Chang and Drs. C.-P. Wu, L.D. Selemon, Y. Li, X.B. Liu, and D. Gelowitz for critical reading of the article.

LITERATURE CITED

- Akintunde A, Buxton DF. 1992. Origins and collateralization of corticospinal, corticopontine, corticorubral and corticostriatal tracts: a multiple retrograde fluorescent tracing study. *Brain Res* 586:208–218.
- Ariav G, Polsky A, Schiller J. 2003. Submillisecond precision of the input-output transformation function mediated by fast sodium dendritic spikes in basal dendrites of CA1 pyramidal neurons. *J Neurosci* 23:7750–7758.
- Bannister NJ, Larkman AU. 1995a. Dendritic morphology of CA1 pyramidal neurons from the rat hippocampus: I. Branching patterns. *J Comp Neurol* 360:150–160.
- Bannister NJ, Larkman AU. 1995b. Dendritic morphology of CA1 pyramidal neurons from the rat hippocampus: II. Spine distributions. *J Comp Neurol* 360:161–171.
- Baranyi A, Szenté MB, Woody CD. 1993. Electrophysiological characterization of different types of neurons recorded *in vivo* in the motor cortex of the cat. I. Patterns of firing activity and synaptic responses. *J Neurophysiol* 69:1850–1864.
- Benavides-Piccione R, Ballesteros-Yanez I, DeFelipe J, Yuste R. 2002. Cortical area and species differences in dendritic spine morphology. *J Neurocytol* 31:337–346.
- Buckmaster PS, Alonso A, Canfield DR, Amaral DG. 2004. Dendritic mor-

- phology, local circuitry, and intrinsic electrophysiology of principal neurons in the entorhinal cortex of macaque monkeys. *J Comp Neurol* 470:317–329.
- Buhl EH, Lubke J. 1989. Intracellular lucifer yellow injection in fixed brain slices combined with retrograde tracing. light and electron microscopy. *Neuroscience* 28:3–16.
- Catsman-Berrevoets CE, Kitai ST. 1981. A search for corticospinal collaterals to thalamus and mesencephalon by means of multiple retrograde fluorescent tracers in cat and rat. *Brain Res* 218:15–33.
- Catsman-Berrevoets CE, Kuypers HGJM. 1978. Differential laminar distribution of corticothalamic neurons projecting to the VL and the center median: an HRP study in the cynomolgus monkey. *Brain Res* 154:359–365.
- Catsman-Berrevoets CE, Lemon RN, Verburch CA, Bentivoglio M, Kuypers HGJM. 1980. Absence of callosal collaterals derived from rat corticospinal neurons. *Exp Brain Res* 39:433–440.
- Chagmac-Amitai Y, Luhman HJ, Prince DA. 1990. Burst generating and regular spiking layer 5 pyramidal neurons of rat neocortex have different morphological features. *J Comp Neurol* 296:598–613.
- Chen W, Zhang JJ, Hu GY, Wu CP. 1996. Electrophysiological and morphological properties of pyramidal and nonpyramidal neurons in the cat motor cortex in vitro. *Neuroscience* 73:39–55.
- Church J, Baimbridge KG. 1991. Exposure to high-PH medium increases the incidence and extent of dye coupling between rat hippocampal CA1 pyramidal neurons in vitro. *J Neurosci* 11:3289–3295.
- Connors BW, Gutnick MJ. 1990. Intrinsic firing patterns of diverse neocortical neurons. *Trends Neurosci* 13:99–104.
- Cowan RL, Wilson CJ. 1994. Spontaneous firing patterns and axonal projections of single corticostriatal neurons in the rat medial agranular cortex. *J Neurophysiol* 71:17–32.
- Dechenes M, Labelle A, Landry P. 1979. Morphological characteristics of slow and fast pyramidal tract cells in the cat. *Brain Res* 178:251–274.
- DeFelipe J, Farinas I. 1992. The pyramidal neurons of the cerebral cortex: morphological and chemical characteristics of the synaptic inputs. *Prog Neurobiol* 39:563–607.
- Deschenes M, Bourassa J, Pinault D. 1994. Corticothalamic projections from layer V cells in rat are collaterals of long-range corticofugal axons. *Brain Res* 664:215–219.
- Donoghue JP, Kitai ST. 1981. A collateral pathway of the rat sensory-motor cortex: an intracellular HRP study. *J Comp Neurol* 201:1–13.
- Ebrahimi A, Pochet R, Roger M. 1992. Topographical organization of the projections from physiologically identified areas of the motor cortex to the striatum in the rat. *Neurosci Res* 14:39–60.
- Elston GN, Rockland KS. 2002. The pyramidal cell of the sensorimotor cortex of the macaque monkey: phenotypic variation. *Cereb Cortex* 12:1071–1078.
- Engert F, Bonhoeffer T. 1999. Dendritic spine changes associated with hippocampal long-term synaptic plasticity. *Nature* 399:66–70.
- Feldman ML. 1984. Morphology of the neocortical pyramidal neuron. In: Peters A, Jones EG, editors. *Cerebral cortex*, vol 1. New York: Plenum Press. p 123–200.
- Feldman ML, Peters A. 1979. A technique for estimating total spine numbers on Golgi-impregnated dendrites. *J Comp Neurol* 188:527–542.
- Franceschetti S, Sancini G, Panzica F, Radici C, Avanzini G. 1998. Postnatal differentiation of firing properties and morphological characteristics in layer V pyramidal neurons of the sensorimotor cortex. *Neurosci* 83:1013–1024.
- Gabbott PLA, Martin KAC, Whitteridge D. 1987. Connections between pyramidal neurons in layer V of cat visual cortex (area 17). *J Comp Neurol* 259:364–381.
- Gao WJ, Li Y, Mao JB, Zheng ZH. 1996. A method of intracellular Lucifer yellow injection in fixed slices combined with retrograde fluorescent tracing. *Chin J Neuroanat* 12:273–276.
- Gerfen CR. 1989. The neostriatal mosaic: striatal patch-matrix organization is related to cortical lamination. *Science* 246:385–388.
- Ghosh S, Fyffe REW, Porter R. 1988. Morphology of neurons in area 4 gamma of the cat's cortex studied with intracellular injection of HRP. *J Comp Neurol* 269:290–312.
- Hallman LE, Schofield BR, Lin CS. 1988. Dendritic morphology and axon collaterals of corticotectal, corticopontine, and callosal neurons in layer V of primary visual cortex of the hooded rat. *J Comp Neurol* 272:149–160.
- Hamada I, Sakai M, Kubota K. 1981a. Morphological differences between fast and slow pyramidal. *Neurosci Lett* 22:233–238.
- Hamada I, Sakai M, Kubota K. 1981b. Morphological differences between fast and slow pyramidal tract neurons in the monkey motor cortex as revealed by intracellular injection of HRP by pressure. *Neurosci Lett* 22:233–238.
- Harris KM, Kater SB. 1994. Dendritic spines: cellular specializations imparting both stability and flexibility to synaptic function. *Annu Rev Neurosci* 17:341–371.
- Hausser M, Mel B. 2003. Dendrites: bug or feature? *Curr Opin Neurobiol* 13:372–383.
- Hausser M, Spruston N, Stuart GJ. 2000. Diversity and dynamics of dendritic signaling. *Science* 290:739–744.
- Holthoff K, Tsay D, Yuste R. 2002. Calcium dynamics of spines depend on their dendritic location. *Neuron* 33:425–437.
- Hubener M, Schwarz C, Bolz J. 1990. Morphological types of projection neurons in layer 5 of cat visual cortex. *J Comp Neurol* 301:655–674.
- Johnston D, Magee JC, Colbert CM, Cristie BR. 1996. Active properties of neuronal dendrites. *Annu Rev Neurosci* 19:165–186.
- Jones EG, Coulter JD, Burton H, Porter R. 1977. Cells of origin and terminal distribution of corticostriatal fibers arising in the sensory-motor cortex of monkeys. *J Comp Neurol* 173:53–80.
- Katz LC. 1987. Local circuitry of identified projection neurons in cat visual cortex brain slices. *J Neurosci* 7:1223–1249.
- Kim HG, Connors BW. 1993. Apical dendrites of the neocortex: correlation between sodium- and calcium-dependent spiking and pyramidal cell morphology. *J Neurosci* 13:5301–5311.
- Konur S, Rabinowitz D, Fenstermaker VL, Yuste R. 2003. Systematic regulation of spine sizes and densities in pyramidal neurons. *J Neurobiol* 56:95–112.
- Labelle A, Deschenes M. 1979. Differential distribution of spines on the apical dendrites of fast and slow pyramidal tract cells in the cat. *Brain Res* 164:309–313.
- Landry P, Wilson CJ, Kitai ST. 1984. Morphological and electrophysiological characteristics of pyramidal tract neurons in the rat. *Exp Brain Res* 57:177–190.
- Larkman AU. 1991a. Dendritic morphology of pyramidal neurons of the visual cortex of the rat: I. Branching patterns. *J Comp Neurol* 306:307–319.
- Larkman AU. 1991b. Dendritic morphology of pyramidal neurons of the visual cortex of the rat: III. Spine distributions. *J Comp Neurol* 306:332–343.
- Larkman AU, Mason A. 1990. Correlations between morphology and electrophysiology of pyramidal neurons in slices of rat visual cortex. I. Establishment of cell classes. *J Neurosci* 10:1407–1414.
- Larkum ME, Zhu JJ, Sakmann B. 1999. A new cellular mechanism for coupling inputs arriving at different cortical layers. *Nature* 398:338–341.
- Liu XB, Zheng ZH, Xi MC, Wu CP. 1991. Distribution of synapses on fast and slow pyramidal tract neurons in the cat. An electron microscopic study. *Brain Res* 545:239–247.
- Macchi G, Bentivoglio M. 1986. The thalamic intralaminar nuclei and the cerebral cortex. In: Peters A, Jones EG, editor. *Cerebral cortex*, vol 5. New York: Plenum Press. p 355–401.
- Magee J, Hoffman D, Colbert C, Johnston D. 1998. Electrical and calcium signaling in dendrites of hippocampal pyramidal neurons. *Annu Rev Physiol* 60:327–346.
- Mainen ZF, Sejnowski TJ. 1996. Influence of dendritic structure on firing pattern in model neocortical neurons. *Nature* 382:363–366.
- Maletic-Savatic M, Malinow R, Svoboda K. 1999. Rapid dendritic morphogenesis in CA1 hippocampal dendrites induced by synaptic activity. *Science* 283:1923–1927.
- Mason A, Larkman AU. 1990. Correlations between morphology and electrophysiology of pyramidal neurons in slices of rat visual cortex. II. Electrophysiology. *J Neurosci* 10:1415–1428.
- McGeorge AJ, Faull RLM. 1989. The organization of the projection from the cerebral cortex to the striatum in the rat. *Neuroscience* 29:503–537.
- Miller MW. 1987. The origin of corticospinal projection neurons in rat. *Exp Brain Res* 67:339–351.
- Peters A, Kaiserman-Aramof IR. 1970. The small pyramidal neuron of the rat cerebral cortex: perikarya, dendrites and spines. *Am J Anat* 127:321–356.
- Poirazi P, Mel BW. 2001. Impact of active dendrites and structural plasticity on the memory capacity of neural tissue. *Neuron* 29:779–796.
- Reyes A. 2001. Influence of dendritic conductances on the input-output properties of neurons. *Annu Rev Neurosci* 24:653–675.

- Rouiller EM, Welker E. 2000. A comparative analysis of the morphology of corticothalamic projections in mammals. *Brain Res Bull* 53:727–741.
- Royce GJ. 1983a. Cells of origin of corticothalamic projections upon the centromedian and parafascicular nuclei in the cat. *Brain Res* 258:11–21.
- Royce GJ. 1983b. Cortical neurons with collateral projections to both the caudate nucleus and the centromedian-parafascicular thalamic complex: a fluorescent retrograde double labeling study in the cat. *Exp Brain Res* 50:157–165.
- Sabatini BL, Maravall M, Svoboda K. 2001. Ca⁺ signaling in dendritic spines. *Curr Opin Neurobiol* 11:349–356.
- Samejima A, Yamamoto T, Oka H. 1987. Two groups of corticofugal neurons identified with the pontine stimulation in the cat parietal association cortex: intracellular HRP study. *Brain Res* 347:117–120.
- Schaefer AT, Larkum ME, Sakmann B, Roth A. 2003. Coincidence detection in pyramidal neurons is tuned by their dendritic branching pattern. *J Neurophysiol* 89:3143–3154.
- Segal M. 1995. Dendritic spines for neuroprotection: a hypothesis. *TINS* 18:468–471.
- Segal M. 2002. Dendritic spines: elementary structural units of neuronal plasticity. *Prog Brain Res* 138:53–59.
- Shepherd GM. 1996. The dendritic spine: a multifunctional integrative unit. *J Neurophysiol* 75:2197–2210.
- Sholl DA. 1953. Dendritic organization in the neurons of the visual and motor cortices of the cat. *J Anat* 87:387–407.
- Trommald M, Jessen V, Andersen P. 1995. Analysis of dendritic spines in rat CA1 pyramidal cells intracellularly filled with a fluorescent dye. *J Comp Neurol* 353:260–274.
- Veinante P, Lavallee P, Deschenes M. 2000. Corticothalamic projections from layer 5 of the vibrissal barrel cortex in the rat. *J Comp Neurol* 424:197–204.
- Vetter P, Roth A, Hausser M. 2001. Propagation of action potentials in dendrites depends on dendritic morphology. *J Neurophysiol* 85:926–937.
- Williams SR, Stuart GJ. 2002. Dependence of EPSP efficacy on synapse location in neocortical pyramidal neurons. *Science* 295:1907–1910.
- Williams SR, Stuart GJ. 2003. Role of dendritic synapse location in the control of action potential output. *Trends Neurosci* 26:147–154.
- Wilson CJ. 1987. Morphology and synaptic connections of crossed corticostriatal neurons in the rat. *J Comp Neurol* 263:567–580.
- Wise SP, Jones EG. 1977. Cells of origin and terminal distribution of descending projections of the rat somatic sensory cortex. *J Comp Neurol* 175:129–158.
- Yamamoto T, Samejima A, Oka H. 1987a. Morphological features of layer V pyramidal neurons in the cat parietal cortex: an intracellular HRP study. *J Comp Neurol* 265:380–390.
- Yamamoto T, Samejima A, Oka H. 1987b. Morphology of layer V pyramidal neurons in the cat primary somatosensory cortex: an intracellular HRP study. *Brain Res* 437:369–374.
- Yamamoto T, Samejima A, Oka H. 1990. The mode of synaptic activation of pyramidal neurons in the cat primary somatosensory cortex: an intracellular HRP study. *Exp Brain Res* 80:12–22.
- Yuste R, Denk W. 1995. Dendritic spines as basic functional units of neuronal integration. *Nature* 375:682–684.
- Yuste R, Majewska A, Holthoff K. 2000. From form to function: calcium compartmentalization in dendritic spines. *Nat Neurosci* 3:653–659.
- Zhang ZW, Deschenes M. 1997. Intracortical axonal projections of lamina VI cells of the primary somatosensory cortex in the rat: a single-cell labeling study. *J Neurosci* 17:6365–6379.
- Zilles K, editor. 1985. *The cortex of the rat. a stereotaxic atlas*. New York: Springer-Verlag.